Assessment of Metal Hydride Reactors as Thermal Management Enhancement of Hydrogen Fuel Cells in Electric Aircraft

Florian Franke[1], Antje Link[2] and Stefan Kazula[3]
German Aerospace Center (DLR), Cottbus, 03046, Germany

Electrified propulsion systems have the potential to reduce the environmental impact of aviation. Hydrogen fuel cells as primary energy supplier are a promising technology to power the electrically-driven propulsors. However, the thermal management of fuel cells is challenging due to their high amount of excess heat energy at a typically low temperature level. This work investigates the cooling potential of metal hydride (MH) reactors to enhance the thermal management system (TMS) of low temperature fuel cells. As a secondary function, the MH reactor can serve as an emergency hydrogen supply. There are two operation concepts of MH reactors considered in this study. In the first operation concept, the MH acts as a heat sink by absorbing some share of the heat of the fuel cell. This decreases the amount of heat to be removed by the TMS. In the second operation concept, the MH reactor operates as a heat pump to enlarge the temperature difference in the heat transfer fluid cycle. This improves the performance of the heat exchanger of the TMS to reject heat to the ambient air. For both operation modes, a sizing of an MH reactor and a heat exchanger is performed to estimate the impact on the TMS. While an exemplary general aviation aircraft serves as calculation example, the results are also applicable to commuter and regional aviation aircrafts. The study shows, that MH reactors have the potential to reduce the size of the heat exchanger significantly. In quasi-continuous heat pump operation, an MH reactor allows a reduction of the heat exchanger dimensions of up to 8 %. If the maximum heat rejection during take-off determines the heat exchanger size, a reduction of even 39% is reasonable when the MH reactor operates as a heat sink.

I. Nomenclature

Symbols

A	=	heat transfer area of the heat exchanger, m²
c_p	=	specific heat capacity, J/kgK
$\dot{m}$	=	mass flow, kg/s
M	=	molar mass, kg/mol
p	=	pressure, Pa
$P_{FC,el}$	=	electrical power of the fuel cell, kW
$\dot{Q}$	=	heat flow, kW
T	=	temperature, °C
U	=	total heat transfer coefficient of the heat exchanger, W/m²K
ΔE_{pot}	=	potential energy difference of the hydrogen pressure, J
$\Delta H_{abs/des}$	=	reaction enthalpy of the metal hydride, kJ/mol$_{H2}$
ΔH_{H2}	=	lower heating value of hydrogen, kJ/g$_{H2}$
ΔT	=	temperature difference, K

[1] Research Associate, Institute of Electrified Aero Engines – Component Technologies.
[2] Research Associate, Institute of Electrified Aero Engines – Architecture of the Propulsion System.
[3] Group Leader, Institute of Electrified Aero Engines – Component Technologies.

$\Delta T_{\mathrm{offset}}$ = temperature offset of the exhaust air to the heat transfer fluid flowing into the heat exchanger, K
$\Delta \vartheta_{\mathrm{a,b}}$ = local temperature differences at the ends of the heat exchanger, K
$\Delta \vartheta_{\mathrm{m}}$ = logarithmic mean temperature difference, K
η = efficiency, %

Recurring indices
abs = absorption of hydrogen
CF = cold fluid
des = desorption of hydrogen
FC = fuel cell
H2 = hydrogen
HF = hot fluid
HX = heat exchanger
in = inlet of the heat exchanger
MHR = metal hydride reactor
out = outlet of the heat exchanger
ref = reference system

II. Introduction

Aviation serves the society by bringing people together and delivering goods over long distances with high reliability and speed. In the future, the environmental impact of air traffic should be reduced in terms of lower greenhouse gas emissions. To achieve the goals of Europe's "Flightpath 2050" and the aviation industry's "Waypoint 2050", a transformation towards hybrid-electric propulsion and sustainable energy sources presents a promising way [1,2]. Hydrogen is a promising energy carrier for future aviation [3,4]. In combination with fuel cells (FC), hydrogen also empowers electrified aero engines to enter the aviation market [1,3].

Although even state-of-the-art components of electrified propulsion systems offer high efficiencies, an extensive amount of heat, in the range of hundreds of kilowatts up to megawatts, is generated due to the high propulsion power requirements. The low temperature level of the components of electrified propulsion is further challenging for the thermal management system (TMS) [5]. The resulting difference between the FC operating temperature and the ambient air on ground is a main challenge, especially for the thermal management of a low temperature polymer electrolyte membrane fuel cell (LT-PEMFC) [6–8].

In conventional kerosene-fueled turbofan aircrafts, a major share of heat exits the turbine with the exhaust gas [9]. To reject further shares of the heat, the following heat sinks are available: ambient air, fan duct air and fuel [5]. In contrast, the number of potential heat sinks is reduced for electrified propulsion systems. For example, fully electric battery-driven powertrains can only use the ambient air as a heat sink. Fully electric fuel-cell-driven powertrains may also use the hydrogen fuel to reject some share of the heat. However, the direct cooling with cryogenic hydrogen may demand unreasonable heat exchanger (HX) dimensions or intermediate cooling loops to prevent surface frost [6]. Also challenges concerning thermomechanical loads and fatigue arise because of the large temperature differences.

A general conflict in the design of TMSs in aviation arises from the highly variable conditions of the ambient air as a heat sink [5,10]. Both the maximum power requirement and the maximum ambient temperature occur for a relatively short time during take-off. When the components of the TMS are designed to these conditions, they will be oversized for most of the aircraft's operation life. By implementing thermal storage systems, the TMS components could be designed for a lower heat load and thus be smaller, lighter and more efficient [5].

Besides the design of the TMS, the storage of hydrogen is another challenge. Although hydrogen exhibits a high gravimetric energy density, it suffers a low volumetric energy density as a gas at ambient conditions. Compressing gaseous hydrogen (CgH2) at high pressures or liquefying hydrogen at cryogenic temperatures are common storage methods to reduce the required volume for the fuel storage. Due to its low weight and its relatively good volume capacities, liquified hydrogen storage seems to be the most promising storage type for aviation. However, the hydrogen losses due to boil-off and the necessary thermal management systems are disadvantageous [3]. Hence, CgH2 storage can be reasonable, especially for general aviation aircrafts [11]. Another hydrogen storage method is storing hydrogen in a solid state, e.g. in metal hydrides (MH). Those MHs form when the hydrogen reacts with metallic compounds. MHs offer the highest possible volumetric storage densities, while their gravimetric hydrogen storage capacity is too low to serve as a competitive primary hydrogen storage system in aviation [3,12].

In addition to hydrogen storage, MH reactors have demonstrated their suitability for high-power thermal applications [12,13]. MHs offer high thermal storage capacities of up to 2 000 kJ/$\mathrm{kg_{MH}}$ and therefore are most suitable

as an additional heat sink [12–14]. Besides such an utilization as a thermal storage material, MH reactors (MHR) can also be used as a heat pump [12–16]. These heat pumps are compact and can be driven by waste heat and by compressed hydrogen [12]. When combined with CgH2 storage systems, MH-based heat pumps can convert the potential energy of the hydrogen tank pressure to thermal energy for heating as well as cooling [17–19]. So far, this potential energy is usually throttled to the FC's supply pressure and therefore lost [20]. By using this potential energy, MH-based thermal devices are environmentally friendly, as they can operate without hazardous refrigerants and require only minor additional amounts of electric energy for their control systems [18,21,22].

The environmentally friendly operation of MHs and their high thermal energy density seem promising for improving the TMS of electrified propulsion systems. This work investigates the potential of MHRs to enhance the TMS of LT-PEMFCs, which are supplied by CgH2. First, the characteristics of conventional TMSs of FC-based propulsion systems are introduced. In addition, the operation behavior of MHs as well as examples of the thermal coupling of MHRs to FCs are described. Subsequently, the sizing method to estimate the potential reduction of the HX dimensions is presented. Finally, two different concepts for integrating an MHR into the aircraft's powertrain are developed and sized. In the first concept, one single MHR works as a heat storage device. In the second concept, two alternating MHRs operate as a heat pump. The sizing enfolds the components of MHR and HX and is performed various ambient temperature levels. As FC powertrains are expected to be less suitable for medium and long haul flights, the evaluation in this study is performed for an exemplary general aviation aircraft while being also applicable to commuter and regional aircrafts [2].

III. State of the Art

As a basis for evaluating the potential of MHRs to improve the thermal management of FC-powered aviation, this chapter describes the challenges for conventional TMS of LT-PEMFCs and presents thermal applications of MHs.

A. TMS of LT-PEMFCs in Aviation

A promising fuel cell type to be used as primary electrical power supply system in electrified aircrafts are LT-PEMFCs, but they require extensive cooling [23]. The power input in form of the enthalpy of the reactant gases into the FC is converted into the electrical power $P_{FC,el}$ with an efficiency of about 40 to 60 % [7,24,25]. The major share of the residual power input is converted into heat as illustrated in Fig. 1. Not all of this thermal power needs to be rejected by the TMS, as some share of the heat also dissipates by natural convection or is used for water vaporization [26,27].

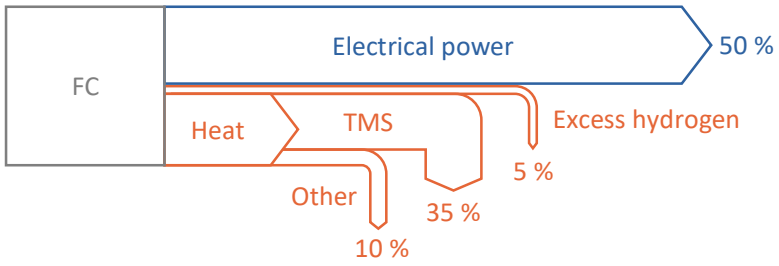

Fig. 1 Energy flows for a PEMFC with an efficiency of 50 % according to Palladino et al. [27].

The FC's TMS typically uses a liquid coolant to pick up the waste heat [23,26,28]. Subsequently, a HX is required to reject the heat to ambient air. Previous investigations have shown a significant contribution of the TMS mass to the total powertrain mass of electrified aircrafts, as the TMS mass can exceed the mass of the corresponding FC [27,29–31]. Besides deteriorating the overall specific power, the extensive TMS of electrified propulsion systems also increases the drag and reduces the available design space [8].

For flight applications, compact HXs, such as plate fin heat exchangers, are suitable due to their minimized combination of mass and volume [32]. Still, the high heat load in concatenation with a low temperature difference to the ambient conditions as a heat sink impose a challenge on HX design, especially during take-off at hottest day conditions [5].

Alternative cooling concepts, as shown by Webber et al. [6], propose an additional heat pump with a vapor compression cycle to increase the heat rejection temperature difference for the TMS of LT-PEMFCs. Thereby, the HX size can be reduced, while increasing the system complexity. The reduced size raises the potential to reduce the drag penalty of the TMS.

B. Metal Hydrides and their Thermal Application

The formation of MHs is described by Eq. (1).

$$\text{metal}_{\text{solid}} + \text{hydrogen}_{\text{gaseous}} \leftrightarrows \text{metal hydride}_{\text{solid}} + \text{heat} \tag{1}$$

Heat is released during the uptake of hydrogen in the metal when forming the MH due to the exothermic characteristic of the absorption process. As the desorption of hydrogen is an endothermic reaction, heat supply is required to release the hydrogen [13]. This enables the thermal application of MHs as a heat source, a heat sink or a heat pump, which is the subject of several studies [12,13,17,22,33].

Synergies in heat exchange can be used when the MHR is coupled to an FC [34]. Several studies investigated the use of the FC's waste heat to maintain the endothermic desorption of the MH and thereby release the necessary hydrogen for reliable FC operation [35–48]. By that, the utilization of the hydrogen storage capacity of the MH is improved as well. In most arrangements, the liquid cooling loop of the FC is therefore extended into the MHR, which is equipped with internal heat transfer elements [38]. Other approaches are either direct coupling of the FC and the MH by heat pipes or placing the MHR into the warm exhaust of air-cooled FC's [38,40,48]. As liquid-cooling is generally mandatory for FCs with high power levels and high power densities, this study focusses on such TMS with a liquid heat transfer fluid (HTF) cycle [26,28,35,49].

By providing the heat to the MH for the endothermic desorption of hydrogen, the MH acts as a heat sink by absorbing a share of 20 % up to 45 % the FC's waste heat, which increases the overall system efficiency [35,38,40,50]. Furthermore, the MHR can also be used to preheat FCs at cold start scenarios, when heat is generated during the absorption of hydrogen from the main hydrogen storage [34,51,52]. MHs are beneficial for such heat storage applications due to their long-lasting storage duration and very high energy densities even superior to phase change materials [12–14,53].

By integrating a set of two MHRs into the hydrogen infrastructure of an FC, a quasi-continuous heat pump operation can be realized [18–21,54]. The working principle of such heat pumps, which are driven by the potential energy of the hydrogen ΔE_{pot}, is illustrated in Fig. 2. The MHRs are working in an alternating manner. While one of the reactors supplies hydrogen to the FC at a low pressure level by desorption, the other reactor regenerates by absorbing hydrogen at a high pressure level from the compressed hydrogen storage. While the regenerating reactor releases heat during absorption $\dot{Q}_{\text{abs}}$ at a high temperature level, the hydrogen supplying reactor requires heat for desorption $\dot{Q}_{\text{des}}$, which can be provided at a lower temperature level. So far, this heat pump operation is investigated to provide a cooling effect for air conditioning purposes [18,20,21,33,54].

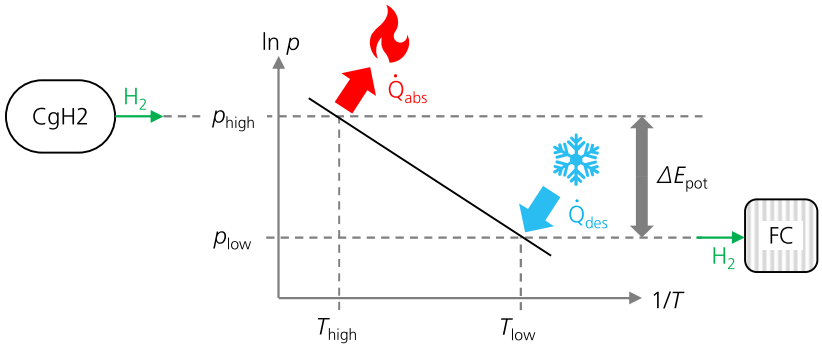

Fig. 2 Working principle of a metal hydride heat pump integrated into the hydrogen infrastructure of a fuel cell (FC) and a gaseous compressed hydrogen storage (CgH2) according to Kölbig et al. [33].

The goal of this study is to determine the potential of MHRs to enhance the TMS of FCs either as a heat sink by absorbing a share of the waste heat or by improving the heat rejection of the HX through enlarging the HTF temperature difference through heat pump operation.

IV. Methodical Approach

For evaluating the potential of MHRs as enhancement of the TMS of an FC-powered propulsion system in aviation, the process according to Fig. 3 has been elaborated and will be applied in the following.

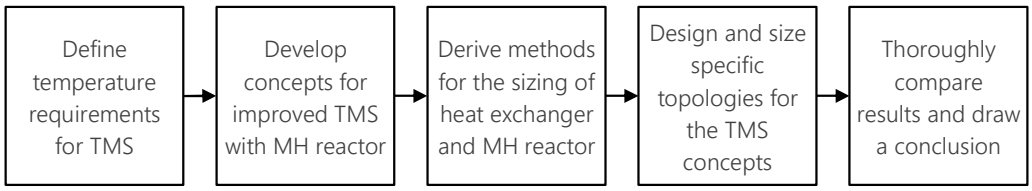

Fig. 3 Applied process to evaluate the potential of MHRs for improving the TMS of an FC.

The specific methods applied for each of these process steps are described in the following subsections. For the evaluation of the improvement achieved by the integration of an MH system, the masses of the HX and of the MHR are considered. The impact of other components like pipes and valves should be investigated during a later design phase if the concepts are viable.

A. Ambient Temperature Requirements in Aviation

The maximum ambient temperature has a significant influence on the sizing of the HX. An overview of temperature requirements in aviation is given in Table 1. The sizing of the HX will be performed within this range from 15 °C to 45 °C to investigate the impact of the ambient temperature.

Table 1 Ambient temperature requirements in aviation.

Temperature Definition	Value	Source
International standard atmosphere (ISA) temperature at sea level	15 °C	[10]
International hot day	40 °C (ISA + 25)	[5]
Maximum temp. for CS-23 aircrafts with reciprocating engine and maximum take-off weight (MTOW) > 2 722 kg or CS-23 aircrafts with turbine engine	38 °C	[55]
Maximum temp. for CS-23 aircrafts with reciprocating engine and MTOW ≤ 2 722 kg	45 °C (ISA + 30)	[55]
Maximum temp. for CS-25 aircrafts	37.8 °C	[56]

B. Concepts for MHR Integration

In this section, two concepts of implementing the MHR into the FC's TMS are developed. To evaluate the additional thermal management capability of those concepts, a comparison to a reference TMS is carried out. The reference TMS consists of a liquid cooled FC system with heat rejection to ambient air. For simplification purposes, all of the FC's heat is rejected by the HX as illustrated in Fig. 4.

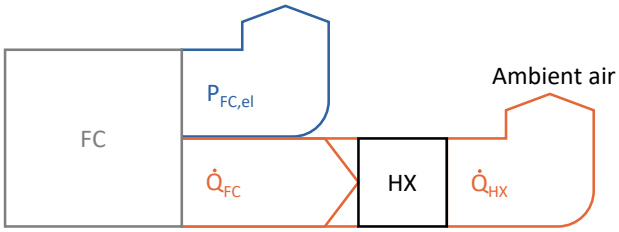

Fig. 4 Heat transfer from fuel cell (FC) to heat exchanger (HX) in the reference TMS.

In concept 1, the heat is handled by the HX in combination with the MHR as illustrated in Fig. 5. The MHR operates as a heat sink and picks up some share of the FC's waste heat for its endothermic desorption of hydrogen.

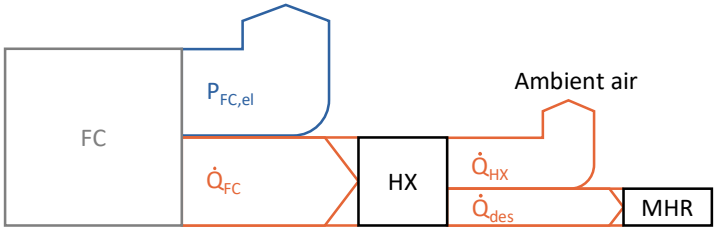

Fig. 5 Concept 1 - Heat transfer from fuel cell (FC) to the heat exchanger (HX) as well as to the metal hydride reactor (MHR) operating as a heat sink.

In this heat sink operation, less heat has to be rejected by the HX. At the same time, the HX has to work with a narrower temperature difference in the HTF as the MHR contributes in cooling down the HTF, while the overall temperature difference, which is limited by the properties of the FC, is therefore not changed. Furthermore, the duration of the cooling effect is limited by the hydrogen capacity of the MHR, as the MH only absorbs heat during the endothermic desorption of hydrogen. Thus, concept 1 is only expected to be beneficial for short-term use during flight mission phases, which require a high-power output, like take-off or climb, and therefore imply a large amount of heat to be rejected [57].

In concept 2, a set of two alternating MHRs operate as a heat pump. The working principle corresponds to the vapor compression cycle heat pump proposed by Webber et al. [6]. Concept 2 is shown in Fig. 6.

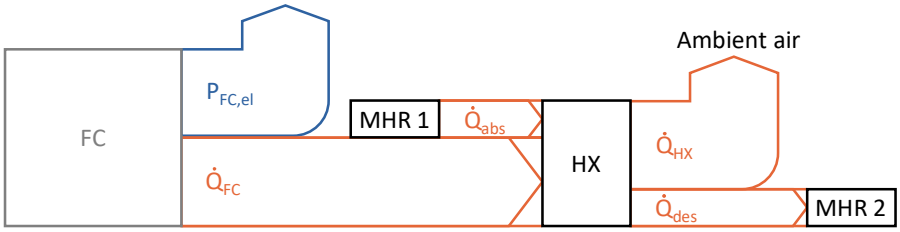

Fig. 6 Concept 2 - Heat transfer from fuel cell (FC) to heat exchanger (HX) with an additional set of two metal hydride reactors (MHR) operating as a heat pump.

In this heat pump operation, the first MHR elevates the temperature of the HTF by heat released through the exothermic absorption of hydrogen. Thereby, the heat rejection temperature difference to the ambient air is increased and the HX size can be reduced, even if the amount of heat, which the HX has to reject, stays nearly constant. Subsequently, the second MHR removes the amount of heat, which was added beforehand by the first MHR, through the endothermic desorption of hydrogen and thus re-establishes the FC's input temperature level.

As an advantage compared to concept 1, the operation duration of the MH heat pump according to concept 2 is not limited. After conversion of the complete hydrogen capacity, both MHRs switch their operating modes and the flow of the HTF is adapted accordingly, so that the second MHR is increasing the HTF temperature and the first MHR re-absorbs the share of the heat. By this alternating operation of the two MHRs, a quasi-continuous operation of the MH heat pump is achieved.

C. Metal Hydride Reactor Sizing Method

To evaluate the MH-enhanced TMS, the thermal power of the MHR has to be calculated. The heat for absorption and desorption $\dot{Q}_{abs/des}$ depends on the hydrogen mass flow $\dot{m}_{H2}$, the molar mass of hydrogen M_{H2} and the reaction enthalpy of the alloy $\Delta H_{abs/des}$ and is calculated by Eq. (2) [18,21,52].

$$\dot{Q}_{abs/des} = \frac{\dot{m}_{H2}}{M_{H2}} \Delta H_{abs/des} \tag{2}$$

The selection of the alloy depends not only on the reaction enthalpy, but also on various other material characteristics like hydrogen storage capacity, thermal conductivity, absorption and desorption kinetics, plateau slope, hysteresis effects, equilibrium pressure, operating temperature, cyclic stability, availability and cost [12,37,38]. To enable the thermal coupling as well as the hydrogen supply to the FC, the MH has to exhibit an equilibrium pressure which is be above the FC's input hydrogen pressure requirement [33,38]. As the equilibrium pressure depends on the temperature, the FC's operating temperature level should be applied for MH selection, as this temperature is provided by the HTF to the MH for desorption. For this study, the alloy $LaNi_{4.85}Al_{0.15}$ is selected. This alloy is commercially available and able to provide high thermal power even for relatively low operating temperatures [17]. $LaNi_{4.85}Al_{0.15}$ is suited to be coupled with a LT-PEMFC as the waste heat of the FC of roughly 80 °C generates a desorption pressure of above 4 bar to supply hydrogen to the FC [53]. The enthalpies of $LaNi_{4.85}Al_{0.15}$ are 31.0 kJ/mol_{H2} for absorption and 33.8 kJ/mol_{H2} for desorption and the usable hydrogen capacity is roughly 1.1 wt.% [53].

The hydrogen mass flow is linked to the FC's electrical power $P_{FC,el}$ and its efficiency η_{FC} according to Eq. (3) [21]. The term ΔH_{H2} refers to the lower heating value of hydrogen of 119.93 kJ/g_{H2} [21,58].

$$P_{FC,el} = \eta_{FC} \Delta H_{H2} \dot{m}_{H2} \tag{3}$$

When the hydrogen mass flows of the FC and the MHR are directly coupled, the theoretical maximum cooling power of the MH $\dot{Q}_{\mathrm{des}}$ can be linked to the FC's electrical power $P_{\mathrm{FC,el}}$ by combining Eq. (2) and Eq. (3), which leads to Eq. (4) [21].

$$\frac{\dot{Q}_{\mathrm{des}}}{P_{\mathrm{FC,el}}} = \frac{\Delta H_{\mathrm{des}}}{M_{\mathrm{H2}} \Delta H_{\mathrm{H2}} \eta_{\mathrm{FC}}} \tag{4}$$

The FC's cooling load $\dot{Q}_{\mathrm{FC}}$ is also a function of the lower heating value of hydrogen ΔH_{H2} and of the FC's efficiency η_{FC} [48,59], which allows to determine the theoretical contribution of the MHR to the necessary cooling load as shown in Eq. (5).

$$\frac{\dot{Q}_{\mathrm{des}}}{\dot{Q}_{\mathrm{FC}}} = \frac{\Delta H_{\mathrm{des}}}{M_{\mathrm{H2}} \Delta H_{\mathrm{H2}} (1 - \eta_{\mathrm{FC}})} \tag{5}$$

It has to be noted that the approach according to Eq. (5) is a simplified assumption because the energy balance of the FC stack is more complex as described in chapter III. The FC's cooling load $\dot{Q}_{\mathrm{FC}}$ represents all the residual power of the reactant gases that is not converted into the electrical power $P_{\mathrm{FC,el}}$. Thus, Eq. (5) neither considers the excess hydrogen nor differentiates between the shares of the waste heat. Furthermore, the thermal insulation of the MHR as well as further components like valves and piping is considered to be ideal in this study, so any heat dissipation from those components by convection or radiation to the environment is not taken into account. The calculations for concept 1 also neglect the heat pickup by the thermal mass of the components. The use of this cooling load $\dot{Q}_{\mathrm{FC}}$ to determine the contribution of the MHR to the TMS and to size the HX leads to conservative results.

According to Eq. (5), the theoretically possible share $\dot{Q}_{\mathrm{des}}/\dot{Q}_{\mathrm{FC}}$, that can be absorbed by the MH, depends on the desorption enthalpy of the alloy ΔH_{des} and increases with higher FC efficiencies η_{FC}. For the example of $LaNi_{4.85}Al_{0.15}$, this theoretical MH's share of heat uptake corresponds to 23 % at an FC efficiency of η_{FC} = 40 % and rises to 35 % at η_{FC} = 60 %. If higher shares are desired, the hydrogen mass flows of MHR and FC have to be uncoupled, for example with the help of a buffer hydrogen storage between those two components. Such buffer would also be beneficial to smoothen the hydrogen supply to the FC [33,38,60]. As such a buffer would cause additional weight, only the direct coupling of the hydrogen mass flows without a buffer is investigated in this study.

Besides the sizing of the thermal power, also the system mass of the MHR is estimated in this study. When used as a heat sink according to concept 1, the mass of the MH depends on the desired operating duration, as the hydrogen capacity of the MH is limited. In regard to the molar mass of hydrogen M_{H2}, the desorption enthalpy of $LaNi_{4.85}Al_{0.15}$ can be converted from 33.8 kJ/mol_{H2} to 16.8 MJ/kg_{H2} [53]. Based on the usable hydrogen capacity of 1.1 wt.%, the thermal energy storage density of $LaNi_{4.85}Al_{0.15}$ is 184.4 kJ/kg_{MH} [53]. This value is used for the estimation of the MH mass of concept 1.

For the heat pump concept 2, thermal losses occur when switching between the two half-cycles of the alternating operation [21]. The transferred specific power strongly depends on the half-cycle time and the ratio of passive reactor mass to active MH mass and may therefore not correlate with the heat of formation for absorption/desorption [20,33]. As this impedes an analytic sizing for concept 2, an empiric approach is used. For the achievable cooling power in relation to the theoretical maximum cooling power of the alloy $\dot{Q}_{\mathrm{des}}$, an efficiency of 81 % is assumed in this study, which has been reported by Weckerle et al. [54]. As this efficiency is linked to the half-cycle duration of the alternating operation, the half-cycle time cannot be arbitrarily reduced to decrease the necessary amount of MH. To estimate the required mass of the MH for the heat pump operation, the specific cooling power of 276 W/kg_{MH}, which was achieved by Weckerle et al. [21], is scaled by the desorption enthalpy of the applied MH alloys. As they used Hydralloy C2 material with a desorption enthalpy of 21.9 kJ/mol_{H2}, a specific cooling power of 426 W/kg_{MH} is assumed in this study for $LaNi_{4.85}Al_{0.15}$ with its higher desorption enthalpy of 33.8 kJ/mol_{H2}. This specific power is expected to be conservative, as the reactor used by Weckerle et al. [21] is not optimized for a low mass, which results in increased switching losses [21].

For the total mass estimation of an MHR, the passive reactor mass has to be calculated besides the active MH mass. In addition to a low mass, also the heat transfer properties of the reactor are crucial to achieve a high mass specific power in thermal applications. So far, a mass ratio of passive reactor mass to active MH mass of 0.97 was achieved for a lightweight reactor with a high specific thermal power [52]. A simplified ratio of 1 is considered in this study as a reasonable approach to estimate passive reactor mass. Thus, the MHR mass is calculated as being twice as much as the MH mass.

D. Heat Exchanger Sizing Method

A single-pass counterflow HX is selected in this study for both ease of calculation and its larger heat transfer potential compared to other flow arrangements [32]. The HX sizing approach follows the logarithmic mean temperature difference sizing of a counterflow HX shown in Eq. (6) with the total heat transfer coefficient U, the heat transfer area A and the logarithmic mean temperature difference $\Delta\vartheta_\mathrm{m}$ across the HX [61,62]. The product UA is later used to characterize the heat exchanger size.

$$\dot{Q}_\mathrm{HX} = UA\Delta\vartheta_\mathrm{m} \tag{6}$$

The logarithmic mean temperature for a counterflow HX is defined as shown in Eq. (7) with the local temperature differences $\Delta\vartheta_\mathrm{a}$ and $\Delta\vartheta_\mathrm{b}$ at both ends of the HX according to Eq. (8) and Eq. (9) [61–63]. The indices HF and CF refer to the associated hot and cold fluids at the in- and outlet of the HX. In this specific application, the hot fluid is the heat transfer fluid (HTF) and the cold fluid is the ambient air flowing through the HX.

$$\Delta\vartheta_\mathrm{m} = \frac{\Delta\vartheta_\mathrm{a} - \Delta\vartheta_\mathrm{b}}{\ln\left(\frac{\Delta\vartheta_\mathrm{a}}{\Delta\vartheta_\mathrm{b}}\right)} \tag{7}$$

$$\Delta\vartheta_\mathrm{a} = T_\mathrm{HF,in} - T_\mathrm{CF,out} \tag{8}$$

$$\Delta\vartheta_\mathrm{b} = T_\mathrm{HF,out} - T_\mathrm{CF,in} \tag{9}$$

To determine the required temperature inputs for the HX sizing of the different concepts, the HX heat flow as well as HTF inlet and outlet temperatures are required for the individual concepts. As those values differ between the investigated concepts, Table 2 provides a summary of the required equations (Eqs. 10 - 13). The use of the MHR as a heat sink according to concept 1 provides two different modelling options depending on whether the fluid enters the HX first and the MHR afterwards as shown in Fig. 5 or vice versa. When the HTF enters the MHR first, the temperature reduction by the MHR would lead to a lower temperature difference to the ambient air in the HX. This leads to lower potential savings in the size of the HX. Therefore, concept 1 is based on the setup, where the HTF flows firstly through the HX and secondly through the MHR.

Table 2 Heat exchanger sizing parameter comparison for reference topology and concepts.

Parameter	Reference	Concept 1	Concept 2	
$\dot{\boldsymbol{Q}}_\mathbf{HX} =$	$\dot{Q}_\mathrm{FC}$	$\dot{Q}_\mathrm{FC} - \dot{Q}_\mathrm{des}$	$\dot{Q}_\mathrm{FC} - \dot{Q}_\mathrm{des} - \dot{Q}_\mathrm{abs}$	(10a-c)
$\boldsymbol{\Delta T}_\mathbf{MHR} =$	0	$\frac{\dot{Q}_\mathrm{des}}{c_\mathrm{p,HF}\cdot\dot{m}_\mathrm{HF}}$	$\frac{\dot{Q}_\mathrm{abs}}{c_\mathrm{p,HF}\cdot\dot{m}_\mathrm{HF}}$	(11a-c)
$\boldsymbol{T}_\mathbf{HF,in} =$	T_FC	T_FC	$T_\mathrm{FC} - \Delta T_\mathrm{MHR}$	(12a-c)
$\boldsymbol{T}_\mathbf{HF,out} =$	$T_\mathrm{FC} - \Delta T_\mathrm{HF}$	$T_\mathrm{FC} - \Delta T_\mathrm{HF} + \Delta T_\mathrm{MHR}$	$T_\mathrm{HF,in} - \frac{\dot{Q}_\mathrm{HX}}{c_\mathrm{p,HF}\cdot\dot{m}_\mathrm{HF}}$	(13a-c)
Note: $\dot{Q}_\mathrm{des} > 0$ and $\dot{Q}_\mathrm{abs} < 0$, which leads to $\Delta T_\mathrm{MHR} > 0$ for concept 1 and $\Delta T_\mathrm{MHR} < 0$ for concept 2				

The calculation of the temperature difference ΔT_MHR, which describes the increase or decrease of the HTF temperature due to the MHR, requires knowledge of the available HTF mass flow $\dot{m}_\mathrm{HF}$. The heat transfer equation as shown in Eq. (14) establishes a general relationship between the heat flow $\dot{Q}$, mass flow $\dot{m}$, specific heat capacity c_p and temperature difference ΔT for heat pickup [62].

$$\dot{Q} = \dot{m}c_\mathrm{p}\Delta T \tag{14}$$

The HTF mass flow is determined for exemplary FC operating conditions. The operating temperature T_{FC} is set to 82 °C with a HTF temperature difference for heat pick-up of ΔT_{HF} = 10 K. The latter has been selected to limit the fuel cell temperature gradient, which can cause cell material degradation [64]. The specific heat capacity of the HTF is assumed with 3500 J/kgK, which is within the range of established LT-PEMFC coolants [65].

For the considered design point of sea level static maximum take-off condition, the air inlet temperature to the HX $T_{CF,in}$ is varied according to the static ambient temperature requirements from Table 1. The air outlet temperature is set via the constant offset ΔT_{offset} = 10 K to the hot fluid inlet temperature of the HX $T_{HF,in}$ as shown in Eq. (15). Such temperature offset assumption for the temperature difference between both fluids is required to limit the heat transfer surface area to prevent unreasonable results.

$$T_{\mathrm{CF,out}} = T_{\mathrm{HF,in}} - \Delta T_{\mathrm{offset}} = T_{\mathrm{HF,in}} - 10\ \mathrm{K} \tag{15}$$

All assessments for the heat sink operation of concept 1 and the heat pump operation of concept 2, are compared to a corresponding reference HX according to Fig. 4. This is initially based on a relative comparison of the achieved reduction in HX size UA to the reference system UA_{ref} as shown in Eq. (16) and Eq. (17).

$$\frac{\Delta UA}{UA_{\mathrm{ref}}} = \frac{UA - UA_{\mathrm{ref}}}{UA_{\mathrm{ref}}} \tag{16}$$

$$\frac{\Delta UA}{UA_{\mathrm{ref}}} = \frac{\dot{Q}_{\mathrm{HX}}\,\Delta\vartheta_{\mathrm{m,ref}}}{\dot{Q}_{\mathrm{HX,ref}}\,\Delta\vartheta_{\mathrm{m}}} - 1 \tag{17}$$

Within literature, there are several HX sizing calculations available for electric propulsion architectures [6,30,31,66]. Evaluating those calculations, the heat flow over the HX is correlated to the predicted HX mass. This introduces the specific heat rejection as a describing parameter. Calculated values for the specific heat rejection range from 1 kW/kg to 6 kW/kg or even 10 kW/kg. Within the provided calculations, a specific heat rejection value of 5 kW/kg is assumed reasonable for the mass estimation of the HX.

V. Results

In this section, specific topologies are developed for integrating the MHR into the FC powertrain for both concepts. Subsequently, the sizing of the TMS of those topologies as well as of the reference case is carried out.

A. Powertrain Topology Design of the Two Concepts

As described in section II, the gravimetric hydrogen storage density of MHs is too low to serve as a primary hydrogen storage system for aircrafts. However, the combination of a CgH2 storage tank with an MHR can be beneficial, as the MH can convert the potential energy of the compressed hydrogen to thermal energy. A suitable setup of an MHR coupled to the CgH2 storage as the FC's hydrogen supply and to the FC's TMS is proposed in Fig. 7.

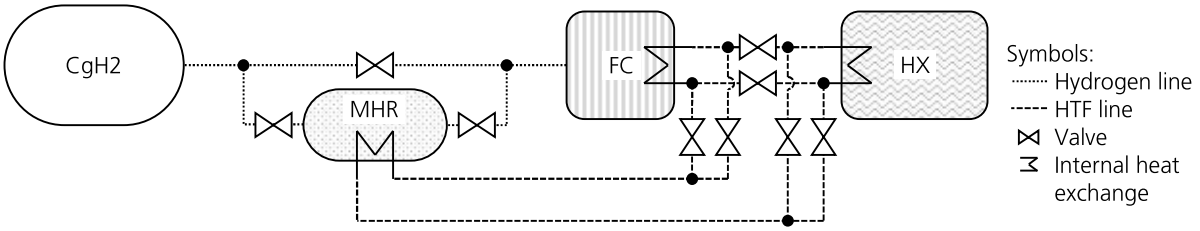

Fig. 7 Simplified topology scheme of an FC powertrain coupled with a single MHR reactor for heat storage according to concept 1.

The valves allow to couple or decouple the MHR with the hydrogen line and the TMS. This topology enables the heat sink operation of the MHR according to concept 1. The hot HTF from the FC may enter the MHR first and flow through the HX afterwards as realized in various studies [39,42–46]. Nevertheless, to minimize the size of the HX, it is reasonable to provide the maximum temperate difference to the ambient air for the HX by guiding the HTF through the HX first and afterwards into the MHR as shown in Fig. 8 a). As the absorption of heat by the MH takes place

during desorption of hydrogen, the MHR is connected to the FC's hydrogen inlet. To maximize the cooling power, no hydrogen is supplied by the CgH2 tank so that the MHR releases the total hydrogen mass flow to operate the FC. The waste heat $\dot{Q}_{FC}$ is transferred to the HTF. Some share of this heat is rejected in the HX ($\dot{Q}_{HX}$), while the residual amount is absorbed by the MHR ($\dot{Q}_{des}$).

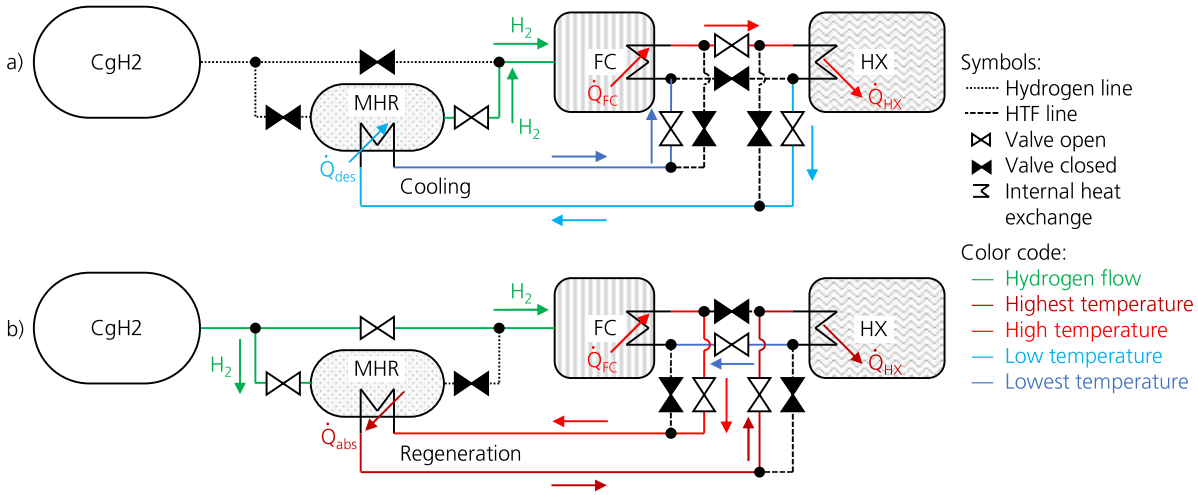

Fig. 8 Operation modes of the FC powertrain topology according to concept 1: a) MHR assists the cooling of the FC, b) Regeneration of the MHR.

After conversion of the complete hydrogen capacity of the MH, the material has to be regenerated by absorbing hydrogen as illustrated in Fig. 8 b). As this is an exothermic reaction and heat is generated, the regeneration should be performed during a low power demand operation of the FC. Moreover, such system can also be used to preheat the FC during a cold start scenario as already proposed by Kazula et al. [34] and by Bürger et al. [52].

For implementation of the two MHRs operating as a heat pump according to concept 2, the topology illustrated in Fig. 9 is proposed. Compared to the topology from Fig. 7, the topology from Fig. 9 adds a second MHR, which is embedded into the hydrogen line as well as into the TMS in parallel with the first reactor.

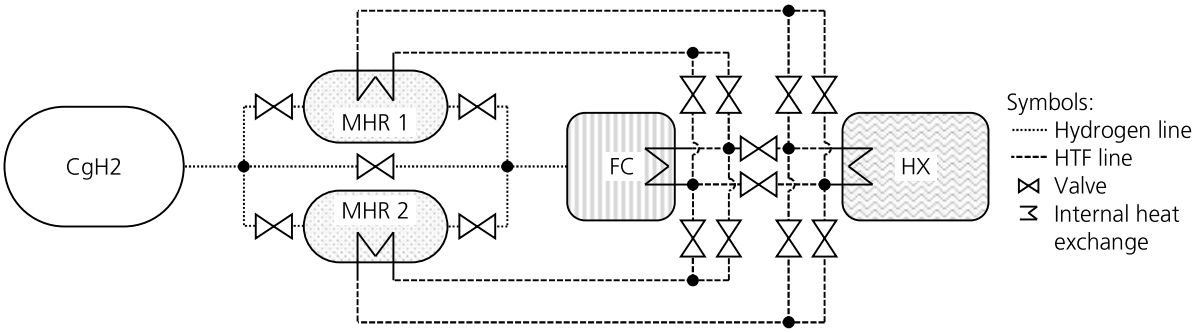

Fig. 9 Simplified scheme of an FC powertrain coupled with two MHRs for alternating heat pump operation according to concept 2.

The operation of both MHRs is alternating. While one MHR is suppling hydrogen to the FC, the other one regenerates by absorbing hydrogen from the CgH2 tank. After complete conversion of the hydrogen capacity of the MH, the first half-cycle is finished. In the second half-cycle, the operating conditions are swapped between the two MHRs. One of the half-cycles of this alternating operation is shown in Fig. 10. While MHR 1 is regenerating by absorbing hydrogen from the CgH2 tank, it increases the temperature level of the HTF before it enters the HX. After the HTF has passed the HX, MHR 2 is roughly removing the same amount of heat, which was added by MHR 1. To achieve this heat uptake, MHR 2 desorbs hydrogen and supplies it to the FC. The HX benefits from the elevated temperature level, as it increases the temperature difference to the ambient air.

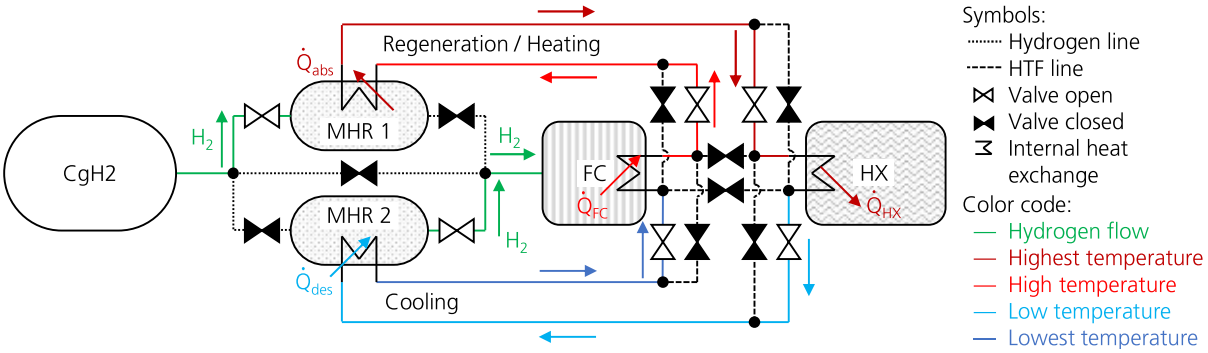

Fig. 10 Half-cycle of the alternating operation of the FC powertrain topology according to concept 2.

B. Sizing Results

The potential of the MH to enhance the TMS of an FC powertrain is assessed for an exemplary twin engine general aviation aircraft with four seats. An overall engine power of 250 kW is chosen for the calculation, which corresponds to the performance of Diamond Aircraft's DA42 [67]. Table 3 shows the resulting cooling load of the FC as well as the corresponding thermal powers of the MHRs and the HX.

Table 3 Theoretical thermal powers of concept 1 and 2 using $LaNi_{4.85}Al_{0.15}$-filled reactors for a 250 kW FC for various FC efficiencies.

Parameter	Value		
FC efficiency η_{FC}	40.0 %	50.0 %	60.0 %
FC cooling load $\dot{Q}_{FC}$	375.0 kW	250.0 kW	166.7 kW
Concept 1:			
MHR heat sink cooling power $\dot{Q}_{des}$	87.4 kW	69.9 kW	58.3 kW
MHR's share on cooling load $\dot{Q}_{des}/\dot{Q}_{FC}$	23.3 %	28.0 %	35.0 %
HX's heat reject thermal power $\dot{Q}_{HX}$	287.6 kW	180.1 kW	108.4 kW
Concept 2:			
MHR's absorption half-cycle heating power $\dot{Q}_{abs}$	- 64.9 kW	- 51.9 kW	- 43.3 kW
MHR's desorption half-cycle cooling power $\dot{Q}_{des}$	70.8 kW	56.6 kW	47.2 kW

These thermal powers are used for the computation of the HTF temperatures and the sizing of the HX according to chapter IV section D. The results of the relative reduction of the HX size $\Delta UA/UA_{ref}$ are shown in Fig. 11. It has to be noted, that these relative results of the HX size are independent of the overall power level and are therefore also valid for larger planes like commuter or regional aircrafts.

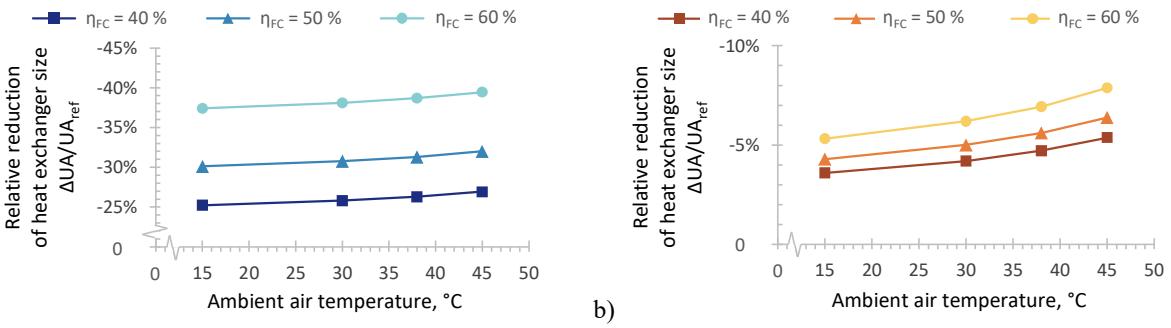

Fig. 11 Relative reduction of the heat exchanger size $\Delta UA/UA_{ref}$ for a) Concept 1 and b) Concept 2.

Concept 1 in Fig. 11 a) offers a higher potential for HX size reduction compared to concept 2 in Fig. 11 b) as the HX has to reject less heat of the overall cooling load. As $\dot{Q}_{abs}$ and $\dot{Q}_{des}$ are nearly the same size in concept 2, the residual amount of heat, that has to be rejected by the HX, changes only insignificantly compared to the reference case. Nevertheless, concept 2 with its benefit of increasing the temperature difference to the ambient air generates also

considerable HX size reduction potential, especially for higher ambient temperatures as the HX becomes less effective. Both concepts show generally higher potential for more efficient FCs.

While concept 2 is able to operate quasi-continuously, concept 1 achieves its potential only for limited operating duration. Due to the maximum hydrogen capacity of the MH, the mass increases with longer target operating durations as illustrated in Fig. 12 a). As the cooling power is limited by the maximum hydrogen consumption of the FC, this MHR mass increase of concept 1 leads to a decreasing specific cooling power of the MHR for longer operating durations according to in Fig. 12 b). Nevertheless, the specific cooling power of concept 1 is too low even for short target operating durations when being compared to the specific power of the HX of 5 kW/kg as described in chapter IV. Although concept 2 enables quasi-continuous operation and its mass is not increasing with operating duration, its generally low specific power presented in chapter IV section C results in a high total MHR mass of 266 kg for an FC efficiency of 50 %, when such a system is sized to operate with the take-off hydrogen mass flow.

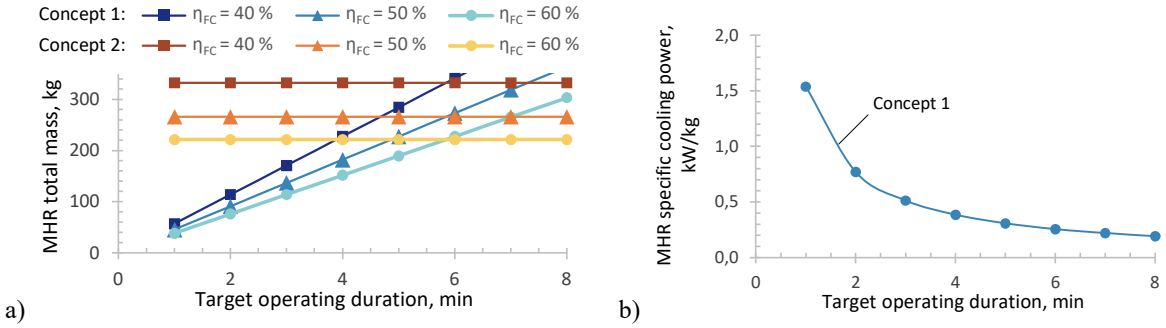

Fig. 12 Influence of the target operating duration: a) Total mass of the MHRs of concept 1 and concept 2 for an FC with 250 kW b) Specific cooling power of the MHR of concept 1.

As a trade-off, a system according to concept 2 can also operate as a heat sink during take-off by desorbing hydrogen from one or both of the MHRs. When desorbing only one MHR, the system can switch to heat pump operation as soon as this MHR is emptied. When desorbing both MHRs, the duration of the heat sink operation is twice as long but one of the MHRs has to be regenerated by absorbing hydrogen before being able to switch to heat pump operation. Such an approach can be reasonable if the aircraft is equipped with two different HXs, consisting of one temporary HX, only used during take-off, and another permanent HX, used during the whole flight mission. The air duct of the temporary HX will be closed during cruise to reduce drag. In such an aircraft as shown in Fig. 13 b), the MHRs will be sized to operate as a heat pump during cruise with its lower hydrogen mass flow. Thereby, the size of the permanent HX can be reduced in the range of Fig. 11 b) to further decrease drag. During take-off, both MHRs will desorb hydrogen in parallel to cope with the higher hydrogen mass flow requirement and to enable the maximum possible cooling power as illustrated in Fig. 13 a). Thereby, also the size of the temporary HX can be reduced, so that the overall reduction of HX size is in the range of Fig. 11 a). Before the air duct of the temporary HX is closed, its heat rejection capacity is used to regenerate one of the MHRs, so the system is able to switch to heat pump operation. The total MHR mass of such system sized to a cruise condition hydrogen mass flow with typically 60 % of take-off power is 145 kg for an FC with 50 % efficiency [68]. This system would be able to operate as a heat sink for above 3 minutes. The relative reduction of the total HX size for take-off conditions at an ambient temperature of 38 °C is 31 % according to Fig. 11 a). For a specific power of the HX of 5 kW/kg as described in chapter IV, this results in absolute HX mass reduction from 50 kg for the 250 kW reference HX to 36 kg for the 180.1 kW HX according to concept 1 in Table 3. This absolute HX mass reduction of 14 kg cannot compensate the mass of 145 kg of the MHRs, which leads to an overall mass increase of 131 kg.

To partly compensate this weight penalty, the MHR could fulfill further functions besides the TMS enhancement. Due to the quasi-continuous, alternating operation, half of the MH's hydrogen capacity is always occupied during heat pump operation. In case of a failure of the primary CgH2 storage, the MHR can serve as a hydrogen emergency supply. For the proposed system of 145 kg total MHR mass, the MH could provide hydrogen for nearly 3 minutes under cruise flight conditions. However, an additional mass of 131 kg is assumed to be too high for an aircraft like the DA42, which exhibits a MTOW of roughly 2 000 kg and a payload of below 600 kg [67].

Since the relative results from Fig. 11 are applicable for larger commuter or regional aircrafts, the absolute mass values may be influenced by scaling effects. While a scalability of the heat exchanging elements inside the MHR and the HX seems reasonable, mass savings at the outer body are expected for larger systems [20]. Nevertheless, a linear scaling of the absolute values of the exemplary general aviation aircraft may be used as a first approach to estimate the absolute MHR and HX masses for commuter or regional aircrafts.

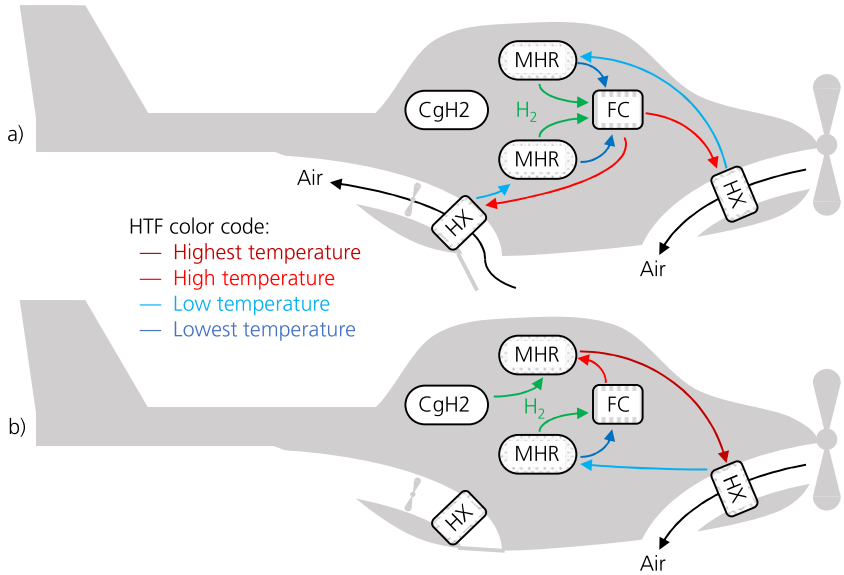

Fig. 13 : Exemplary aircraft with two HXs and MHRs: a) Take-off condition with both HXs in operation and both MHRs as heat sink, b) Cruise condition with only one HX in operation and MHRs as heat pump.

VI. Conclusion

In this study, two concepts of implementing an MHR to enhance the TMS of an FC powertrain were developed. In concept 1, the MHR operates as a heat sink and absorbs some share of the FC's waste heat. In concept 2, a set of two alternating MHRs operate as a heat pump to elevate the temperature of the HTF to increase the heat rejection temperature difference to the ambient air. Subsequently, specific topologies were developed for both concepts to integrate the MHRs into an FC powertrain. Finally, a sizing of the MHR and the HX was performed for various ambient temperature levels.

If the maximum heat rejection during take-off and climb determines the HX size, the implementation of an MHR as a heat sink can lead to a 39 % reduction of the HX dimensions. However, such an application as a heat sink is only recommended as a short-time cooling booster, as the specific cooling power of the MHR decreases with increasing operating duration. The implementation of an MHR as a heat pump is not limited in operating duration. Such system can achieve an 8 % reduction of the HX dimensions.

However, the reduction of HX mass cannot compensate the additional mass of the MHR. To minimize the impact of the additional weight caused by an MH system, the integration of further functions to MHRs, like their potential to store hydrogen for emergency cases, should be considered in future studies. In addition, the potential of a reduced fuel consumption due to the lower drag of the TMS of the aircraft should be investigated. This way, MHRs could become an enabling technology for hydrogen FC-powered propulsion systems in aviation.

Acknowledgments

We wish to acknowledge Inga Bürger, Alexander Wimmer, Markus Kordel, Martin Staggat and Lars Enghardt for their cooperativeness and the fruitful discussions about metal hydrides and their potential applications.

References

[1] Darecki, M., King, I., Edelstenne, C., Ky, P., Enders, T., et al., "Flightpath 2050: Europe's Vision for Aviation; Report of the High-level Group on Aviation Research," 2011.

[2] ATAG - Air Transportation Action Group, "Waypoint 2050: An Air Transport Action Group Project," 2020.

[3] Baroutaji, A., Wilberforce, T., Ramadan, M., and Olabi, A. G., "Comprehensive Investigation on Hydrogen and Fuel Cell Technology in the Aviation and Aerospace Sectors," *Renewable and Sustainable Energy Reviews*, Vol. 106, 2019, pp. 31–40.

[4] Bray, R., Burrows, E., and Hadnum, L., "FlyZero: Aircraft-Systems," Aerospace Technology Institute FZO-AIR-REP-0013, 2022.

[5] Haran, K., Madavan, N., and O'Connell, T. C., *Electrified Aircraft Propulsion. Powering the Future of Air Transportation,* Cambridge University Press, Cambridge, 2022.

[6] Webber, H., Llambrich, J., and Davoudi, H., "FlyZero: Thermal-Management-Roadmap-Report," Aerospace Technology Institute FZO-PPN-COM-0019, 2022.
[7] Kazula, S., de Graaf, S., and Enghardt, L., "Review of Fuel Cell Technologies and Evaluation of their Potential and Challenges for Electrified Propulsion Systems in Commercial Aviation," *GPPS 2022 European Technical Conference,* GPPS, Chania, 2022.
[8] Hadnum, L., Pacey, M., and Milne, K., "FlyZero: Technology-Roadmaps," Aerospace Technology Institute FZO-IST-MAP-0012, 2022.
[9] Tuzcu, H., Sohret, Y., and Caliskan, H., "Energy, Environment and Enviroeconomic Analyses and Assessments of the Turbofan Engine Used in Aviation Industry," *Environmental Progress & Sustainable Energy*, Vol. 40, No. 3, 2021. doi: 10.1002/ep.13547.
[10] Matthews, C., *Aeronautical Engineer's Data Book,* Butterworth-Heineman, Oxford, 2002.
[11] APUS Group, "APUS i-2: The Zero Emission GA Aircraft," URL: https://apus-zero.de/wp-content/uploads/2021/09/APUS_i-2_20210901.pdf [retrieved 8 November 2022].
[12] Muthukumar, P., Kumar, A., Raju, N. N., Malleswararao, K., and Rahman, M. M., "A Critical Review on Design Aspects and Developmental Status of Metal Hydride Based Thermal Machines," *International Journal of Hydrogen Energy*, Vol. 43, No. 37, 2018, pp. 17753–17779.
doi: 10.1016/j.ijhydene.2018.07.157.
[13] Bhuiya, M. M. H., Kumar, A., and Kim, K. J., "Metal Hydrides in Engineering Systems, Processes, and Devices: A Review of Non-storage Applications," *International Journal of Hydrogen Energy*, Vol. 40, No. 5, 2015, pp. 2231–2247. doi: 10.1016/j.ijhydene.2014.12.009.
[14] Yang, F. S., Wang, G. X., Zhang, Z. X., Meng, X. Y., and Rudolph, V., "Design of the Metal Hydride Reactors – a Review on the Key Technical Issues," *International Journal of Hydrogen Energy*, Vol. 35, No. 8, 2010, pp. 3832–3840. doi: 10.1016/j.ijhydene.2010.01.053.
[15] Satheesh, A., and Muthukumar, P., "Performance Investigations of a Single-stage Metal Hydride Heat Pump," *International Journal of Hydrogen Energy*, Vol. 35, No. 13, 2010, pp. 6950–6958.
doi: 10.1016/j.ijhydene.2010.04.043.
[16] Payá, J., Linder, M., Mertz, R., and Corberán, J. M., "Analysis and Optimization of a Metal Hydride Cooling System," *International Journal of Hydrogen Energy*, Vol. 36, No. 1, 2011, pp. 920–930.
doi: 10.1016/j.ijhydene.2010.08.112.
[17] Kölbig, M., Bürger, I., and Linder, M., "Thermal Applications in Vehicles Using Hydralloy C5 in Single and Coupled Metal Hydride Systems," *Applied Energy*, Vol. 287, 2021.
[18] Hegner, R., and Weckerle, C., "Klimatisierungsaggregat auf Metallhydridbasis für Elektrofahrzeuge mit Batterie oder Brennstoffzelle," *ATZ - Automobiltechnische Zeitschrift*, Vol. 122, No. 1, 2020, pp. 82–86.
doi: 10.1007/s35148-019-0161-5.
[19] Weckerle, C., Bürger, I., and Linder, M., "Numerical Optimization of a Plate Reactor for a Metal Hydride Open Cooling System," *International Journal of Hydrogen Energy*, Vol. 44, No. 31, 2019, pp. 16862–16876.
doi: 10.1016/j.ijhydene.2019.04.260.
[20] Weckerle, C., Bürger, I., and Linder, M., "Novel Reactor Design for Metal Hydride Cooling Systems," *International Journal of Hydrogen Energy*, Vol. 42, No. 12, 2017, pp. 8063–8074.
doi: 10.1016/j.ijhydene.2017.01.066.
[21] Weckerle, C., Nasri, M., Hegner, R., Linder, M., and Bürger, I., "A Metal Hydride Air-conditioning System for Fuel Cell Vehicles – Performance Investigations," *Applied Energy*, Vol. 256, 2019, p. 113957.
doi: 10.1016/j.apenergy.2019.113957.
[22] Muthukumar, P., and Groll, M., "Metal Hydride Based Heating and Cooling Systems: A Review," *International Journal of Hydrogen Energy*, Vol. 35, No. 8, 2010, pp. 3817–3831.
doi: 10.1016/j.ijhydene.2010.01.115.
[23] SAE, "Fuel Cell Vehicle Thermal Management," SAE J3193, 2021.
[24] Bhatti, W., Wu, W., Doyle, F., Llambrich, J., Webber, H., et al., "FlyZero: Fuel-Cells-Roadmap-Report," Aerospace Technology Institute FZO-PPN-COM-0033, 2022.
[25] U.S. Department of Transportation, "Energy Supply Device Aviation Rulemaking Committee: Final Report," DOT/FAA/TC-19/16, 2017.
[26] Bargal, M. H., Abdelkareem, M. A., Tao, Q., Li, J., Shi, J., et al., "Liquid Cooling Techniques in Proton Exchange Membrane Fuel Cell Stacks: A Detailed Survey," *Alexandria Engineering Journal*, Vol. 59, No. 2, 2020, pp. 635–655. doi: 10.1016/j.aej.2020.02.005.
[27] Palladino, V., Jordan, A., Bartoli, N., Schmollgruber, P., Pommier-Budinger, V., et al., "Preliminary Studies of a Regional Aircraft with Hydrogen-based Hybrid Propulsion," *AIAA Aviation 2021 Forum,* AIAA, Reston, Virginia, 2021.
[28] Zhang, G., and Kandlikar, S. G., "A Critical Review of Cooling Techniques in Proton Exchange Membrane Fuel Cell Stacks," *International Journal of Hydrogen Energy*, Vol. 37, No. 3, 2012, pp. 2412–2429.
doi: 10.1016/j.ijhydene.2011.11.010.
[29] Lents, C. E., "Impact of Weight, Drag and Power Demand on Aircraft Energy Consumption," *AIAA Propulsion and Energy 2021 Forum,* AIAA, Reston, Virginia, 2021.

[30] Link, A., Ludowicy, J., and Staggat, M., "Assessment of a Serial Cooling Concept for HTPEM Fuel Cell Systems for Aviation Applications," *33rd Congress of the International Council of Aerospace Sciences,* The International Council of Aerospace Sciences, Stockholm, 2022.
[31] Gkoutzamanis, V. G., Tsentis, S. E., Valsamis Mylonas, O. S., Kalfas, A. I., Kyprianidis, K. G., et al., "Thermal Management System Considerations for a Hybrid-Electric Commuter Aircraft," *Journal of Thermophysics and Heat Transfer*, Vol. 36, No. 3, 2022, pp. 650–666. doi: 10.2514/1.T6433.
[32] Shah, R. K., and Sekulić, D. P., *Fundamentals of Heat Exchanger Design,* John Wiley & Sons, Hoboken NJ, 2003.
[33] Kölbig, M., Weckerle, C., Linder, M., and Bürger, I., "Review on Thermal Applications for Metal Hydrides in Fuel Cell Vehicles: Operation Modes, Recent Developments and Crucial Design Aspects," *Renewable and Sustainable Energy Reviews*, Vol. 162, 2022, p. 112385. doi: 10.1016/j.rser.2022.112385.
[34] Kazula, S., de Graaf, S., and Enghardt, L., "Preliminary Safety Assessment of PEM Fuel Cell Systems for Electrified Propulsion Systems in Commercial Aviation," *32nd European Safety and ReliabilityConference (ESREL 2022),* Research Publishing, Dublin, 2022.
[35] Nguyen, H. Q., and Shabani, B., "Review of Metal Hydride Hydrogen Storage Thermal Management for Use in the Fuel Cell Systems," *International Journal of Hydrogen Energy*, Vol. 46, No. 62, 2021, pp. 31699–31726. doi: 10.1016/j.ijhydene.2021.07.057.
[36] Röntzsch, L., and Heubner, F., "Metal Hydride Technology," URL: https://www.ifam.fraunhofer.de/content/dam/ifam/de/documents/dd/Infobl%C3%A4tter/metal_hydride_technology_fraunhofer_ifam_dresden.pdf [retrieved 4 January 2022].
[37] Dornheim, M., and Moreno-Piraján, J. C. (eds.), *Thermodynamics - Interaction Studies - Solids, Liquids and Gases. Interaction Studies - Solids, Liquids, Gases,* IntechOpen, 2011.
[38] Lototskyy, M. V., Tolj, I., Pickering, L., Sita, C., Barbir, F., et al., "The Use of Metal Hydrides in Fuel Cell Applications," *Progress in Natural Science: Materials International*, Vol. 27, No. 1, 2017, pp. 3–20. doi: 10.1016/j.pnsc.2017.01.008.
[39] Mori, D., Hirose, K., Haraikawa, N., Takiguchi, T., Shinozawa, T., et al., "High-pressure Metal Hydride Tank for Fuel Cell Vehicles," SAE 2007-01-2011, 2007.
[40] Tetuko, A. P., Shabani, B., and Andrews, J., "Passive Fuel Cell Heat Recovery Using Heat Pipes to Enhance Metal Hydride Canisters Hydrogen Discharge Rate: An Experimental Simulation," *Energies*, Vol. 11, No. 4, 2018, p. 915. doi: 10.3390/en11040915.
[41] Colozza, A. J., and Kohout, L., "Hydrogen Storage for Aircraft Applications Overview," NASA/CR-2002-211867, 2002.
[42] Heung, L. K., Motyka, T., and Summers, W. A., "Hydrogen Storage Development for Utility Vehicles," U.S. Department of Energy, 2001.
[43] Hwang, J. J., and Chang, W. R., "Characteristic Study on Fuel Cell/Battery Hybrid Power System on a Light Electric Vehicle," *Journal of Power Sources*, Vol. 207, 2012, pp. 111–119. doi: 10.1016/j.jpowsour.2012.02.008.
[44] Hsiao, D.-R., Huang, B.-W., and Shih, N.-C., "Development and Dynamic Characteristics of Hybrid Fuel Cell-powered Mini-train System," *International Journal of Hydrogen Energy*, Vol. 37, No. 1, 2012, pp. 1058–1066. doi: 10.1016/j.ijhydene.2011.02.121.
[45] Khaitan, S. K., and Raju, M., "Discharge Dynamics of Coupled Fuel Cell and Metal Hydride Hydrogen Storage Bed for Small Wind Hybrid Systems," *International Journal of Hydrogen Energy*, Vol. 37, No. 3, 2012, pp. 2344–2352. doi: 10.1016/j.ijhydene.2011.10.098.
[46] Førde, T., Eriksen, J., Pettersen, A. G., Vie, P., and Ulleberg, Ø., "Thermal Integration of a Metal Hydride Storage Unit and a PEM Fuel Cell Stack," *International Journal of Hydrogen Energy*, Vol. 34, No. 16, 1 Jan. 2009, pp. 6730–6739. doi: 10.1016/j.ijhydene.2009.05.146.
[47] Liu, Z., Li, Y., Bu, Q., Guzy, C. J., Li, Q., et al., "Novel Fuel Cell Stack with Coupled Metal Hydride Containers," *Journal of Power Sources*, Vol. 328, 2016, pp. 329–335. doi: 10.1016/j.jpowsour.2016.07.096.
[48] Tetuko, A. P., Shabani, B., and Andrews, J., "Thermal Coupling of PEM Fuel Cell and Metal Hydride Hydrogen Storage Using Heat Pipes," *International Journal of Hydrogen Energy*, Vol. 41, No. 7, 2016, pp. 4264–4277. doi: 10.1016/j.ijhydene.2015.12.194.
[49] O'Hayre, R., Cha, S.-W., Colella, W., and Prinz, F. B., *Fuel Cell Fundamentals,* John Wiley & Sons, Inc, Hoboken, NJ, USA, 2016.
[50] Lee, K. in, Chung, D. K., Park, M. S., and Chu, C. N., "The Development of a Cylindrical Proton Exchange Membrane Fuel Cell with an Integrated Metal-hydride Container," *International Journal of Precision Engineering and Manufacturing*, Vol. 14, No. 6, 2013, pp. 1065–1070. doi: 10.1007/s12541-013-0143-6.
[51] Dieterich, M., Bürger, I., and Linder, M., "Open and Closed Metal Hydride System for High Thermal Power Applications: Preheating Vehicle Components," *International Journal of Hydrogen Energy*, Vol. 42, No. 16, 2017, pp. 11469–11481. doi: 10.1016/j.ijhydene.2017.03.024.

[52] Bürger, I., Sourmelis Terzopoulos, V. E., Kretschmer, C., Kölbig, M., Brack, C., et al., "Lightweight Reactor Design by Additive Manufacturing for Preheating Applications Using Metal Hydrides," *International Journal of Hydrogen Energy*, Vol. 46, No. 56, 2021, pp. 28686–28699. doi: 10.1016/j.ijhydene.2021.06.091.
[53] Kölbig, M., Bürger, I., and Linder, M., "Characterization of Metal Hydrides for Thermal Applications in Vehicles below 0 °C," *International Journal of Hydrogen Energy*, Vol. 44, No. 10, 2019, pp. 4878–4888. doi: 10.1016/j.ijhydene.2018.12.116.
[54] Weckerle, C., Nasri, M., Hegner, R., Bürger, I., and Linder, M., "A Metal Hydride Air-conditioning System for Fuel Cell Vehicles – Functional Demonstration," *Applied Energy*, Vol. 259, 2020, pp. 1–14. doi: 10.1016/j.apenergy.2019.114187.
[55] European Aviation Safety Agency, "Certification Specifications and Acceptable Means of Compliance for Normal, Utility, Aerobatic, and Commuter Category Aeroplanes," CS-23 Amendment 4, 2015.
[56] European Aviation Safety Agency, "Certification Specifications and Acceptable Means of Compliance for Large Aeroplanes," CS-25 Amendment 27, 2015.
[57] Boll, M., Corduan, M., Biser, S., Filipenko, M., Pham, Q. H., et al., "A Holistic System Approach for Short Range Passenger Aircraft with Cryogenic Propulsion System," *Superconductor Science and Technology*, Vol. 33, No. 4, 2020, p. 44014. doi: 10.1088/1361-6668/ab7779.
[58] Arat, H. T., and Sürer, M. G., "State of Art of Hydrogen Usage as a Fuel on Aviation," *European Mechanical Science*, Vol. 2, No. 1, 2017, pp. 20–30. doi: 10.26701/ems.364286.
[59] Larminie, J., and Dicks, A., *Fuel Cell Systems Explained,* 2nd ed., John Wiley & Sons Ltd., Chichester, 2003.
[60] Lototskyy, M., Tolj, I., Klochko, Y., Davids, M. W., Swanepoel, D., et al., "Metal Hydride Hydrogen Storage Tank for Fuel Cell Utility Vehicles," *International Journal of Hydrogen Energy*, Vol. 45, No. 14, 2020, pp. 7958–7967. doi: 10.1016/j.ijhydene.2019.04.124.
[61] Lienhard, IV, John H., and Lienhard, V, John H., *A Heat Transfer Textbook,* 5th ed., Phlogiston Press, 2020.
[62] Wagner, W., *Wärmeübertragung. Grundlagen,* 7th ed., Vogel Buchverlag, Würzburg, 2011.
[63] VDI-Gesellschaft Verfahrenstechnik und Chemieingenieurwesen, *VDI Heat Atlas,* 2nd ed., Springer, Berlin, New York, Heidelberg, London, Dordrecht, 2010.
[64] Dicks, A., and Rand, D. A. J., *Fuel Cell Systems Explained,* 3rd ed., John Wiley & Sons Ltd., Chichester, 2018.
[65] Dynalene Inc., "Dynalene FC Series Technical Data Sheet: Low Electrical Conductivity, Water-based Fuel Cell Coolants with Nanoparticles," URL: https://www.dynalene.com/wp-content/uploads/2020/08/Dynalene-FC-Tech-Data-Sheet-Rev1.pdf [retrieved 2 May 2023].
[66] Chapman, J. W., Schnulo, S. L., and Nitzsche, M. P., "Development of a Thermal Management System for Electrified Aircraft," *AIAA SciTech Forum*, Orlando, 2020.
[67] Diamond Aircraft, "DA42-VI: The Definition of Perfection," URL: https://www.diamondaircraft.com/en/private-owners/aircraft/da42/tech-specs/ [retrieved 8 November 2022].
[68] Colpan, C. O., and Kovač, A. (eds.), *Fuel Cell and Hydrogen Technologies in Aviation,* Springer International Publishing, Cham, 2022.